

On Linear Learning with Manycore Processors

Eliza Wszola
eliza.wszola@inf.ethz.ch
Department of Computer Science
ETH Zurich
Zurich, Switzerland

Martin Jaggi
martin.jaggi@epfl.ch
School of Computer and Communication Sciences
EPFL
Lausanne, Switzerland

Celestine Mender-Dünner
cdu@zurich.ibm.com
IBM Research
Zurich, Switzerland

Markus Püschel
pueschel@inf.ethz.ch
Department of Computer Science
ETH Zurich
Zurich, Switzerland

ABSTRACT

A new generation of manycore processors is on the rise that offers dozens and more cores on a chip and, in a sense, fuses host processor and accelerator. In this paper we target the efficient training of generalized linear models on these machines. We propose a novel approach for achieving parallelism which we call Heterogeneous Tasks on Homogeneous Cores (HTHC). It divides the problem into multiple fundamentally different tasks, which themselves are parallelized. For evaluation, we design a detailed, architecture-cognizant implementation of our scheme on a recent 72-core Knights Landing processor that is adaptive to the cache, memory, and core structure. Experiments for Lasso and SVM with different data sets show a speedup of typically an order of magnitude compared to straightforward parallel implementations in C++.

KEYWORDS

Manycore, coordinate descent, performance, SVM, Lasso

1 INTRODUCTION

The evolution of mainstream computing systems has moved from the multicore to the manycore area. This means that a few dozen to even hundreds of cores are provided on a single chip, packaged with up to hundreds of gigabytes of memory at high bandwidth. Examples include Intel Xeon Phi (up to 72 cores), ARM ThunderX2 (64 cores), Qualcomm Centriq 2400 (48 cores), and of course GPUs (100s of cores). One declared target of the recent generation of manycores is machine learning and one exciting trend is the move from accelerators (like GPUs) to standalone manycore processors that remove the burden of writing two types of code and enable easier integration with applications and legacy code. However, the efficient mapping of the required mathematics to manycores is a difficult task as compilers have inherent limitations to perform this task given straightforward C (or worse, Java, Python, etc.) code, a problem that has been known already for the earlier, simpler multicore and single core systems [31]. Challenges include vector instruction sets, deep cache hierarchies, non-uniform memory architectures, and efficient parallelization. Much work has been devoted to efficient learning and inference of neural nets on GPUs [1, 10, 19, 36, 42] but other domains of machine learning have received less attention.

The challenge we address in this paper is how to map machine learning workloads to manycore processors. We focus on recent standalone manycores and the important task of training generalized linear machine learning models as used for regression, classification, and feature selection. Our core contribution is to show that in contrast to prior approaches, which assign the same kind of subtask to each core, we can achieve significantly better overall performance and adaptivity to the system resources, by distinguishing between two fundamentally different tasks. A subset of the cores will be assigned task \mathcal{A} that only reads the model parameters, while the other subset of cores will perform task \mathcal{B} that updates them. So in the manycore setting, while the cores are *homogeneous*, we show that assigning them *heterogeneous* tasks results in improved performance and use of compute, memory, and cache resources. The adaptivity of our approach is particularly crucial; the best number and assignment of threads can be adapted to the computing platform and the problem at hand.

Contributions. We make the following contributions:

- (1) We describe a scheme, composing of two heterogeneous tasks, running in parallel on homogeneous manycore architectures, in order to train generalized linear models. We call it Heterogeneous Tasks on Homogeneous Cores (HTHC).
- (2) We provide a complete, performance-optimized implementation of HTHC on a 72-core Intel Xeon Phi processor. We describe the challenges of parallelizing both tasks and their solutions. Our code will be made publicly available.
- (3) We present a model for choosing the best distribution of threads for each task with respect to the machine's memory system. We demonstrate that with explicit control over parallelism our approach provides an order of magnitude speedup over a straightforward OpenMP implementation.
- (4) We show that our code, on a single manycore processor, is competitive with the state-of-the-art implementation of a similar approach on a heterogeneous system with CPU and GPU of 1500 GPU cores, and achieves up to an order of magnitude speedup when comparing against state-of-the-art homogeneous implementations on the same processor.

2 PROBLEM STATEMENT & BACKGROUND

This section details the considered problem class, provides necessary background on coordinate selection and introduces our target platform: the Intel Knights Landing (KNL) manycore processor.

2.1 Problem specification

We focus on the training of generalized linear models (GLMs) which can be expressed as the following optimization task:

$$\min_{\alpha \in \mathbb{R}^n} \mathcal{F}(\alpha) := f(D\alpha) + \sum_{i \in [n]} g_i(\alpha_i), \quad (1)$$

where $[n] = \{1, \dots, n\}$, f and g_i are convex functions, and $\alpha \in \mathbb{R}^n$ is the model to be learned from the training data matrix $D \in \mathbb{R}^{d \times n}$ with columns $\mathbf{d}_1, \dots, \mathbf{d}_n$. In addition, f is assumed to be smooth. This general setup covers many widely applied machine learning models including logistic regression, support vector machines (SVM), and sparse models such as Lasso and elastic-net.

The models of this form have two important characteristics. First, since $g = \sum_i g_i(\alpha_i)$ is separable, it is possible to perform updates on different column of the data matrix separately. In particular, we can use stochastic coordinate descent (SCD) to process the data set coordinate-wise. This approach can be extended to batches. Second, importance measures for individual coordinates are available. Such measures depend either on the dataset, the current model parameters or both. They can be used for the selection of important coordinates during coordinate descent, speeding up overall convergence, either by deriving sampling probabilities (importance sampling) or by simply picking the parameters with the highest importance score (greedy approach).

2.2 Duality-gap based coordinate selection

A particular measure of coordinate-wise importance that we will adopt in our method, is the coordinate-wise duality gap certificate proposed by Dünner et al. [15]. The authors have shown that choosing model parameters to update based on their contribution to the duality gap provides faster convergence than random selection and classical importance sampling [48].

Let g_i^* denote the convex conjugates of g_i . Then, the duality gap (see [6]) of our objective (1) can be determined as

$$\begin{aligned} \text{gap}(\alpha; \mathbf{w}) &= \sum_{i \in [n]} \text{gap}_i(\alpha_i; \mathbf{w}), \quad \text{with} \\ \text{gap}_i(\alpha_i; \mathbf{w}) &:= \alpha_i \langle \mathbf{w}, \mathbf{d}_i \rangle + g_i(\alpha_i) + g_i^*(-\langle \mathbf{w}, \mathbf{d}_i \rangle), \end{aligned} \quad (2)$$

where the model vector α, \mathbf{w} are related through the primal-dual mapping $\mathbf{w} := \nabla f(D\alpha)$. Importantly, knowing the parameters $\alpha; \mathbf{w}$, it is possible to calculate the duality gap values (2) for every $i \in [n]$ independently and thus in parallel. In our implementation, we introduce the shared vector $\mathbf{v} = D\alpha$ from which \mathbf{w} can be computed using a simple linear transformation for many problems of interest.

2.3 The Knights Landing architecture

Intel Knights Landing (KNL) is a manycore processor architecture used in the second generation Intel Xeon Phi devices, the first host processors, i.e., not external accelerators, offered in this line. It provides both high performance (with machine learning as one

declared target) and x86 backwards compatibility. A KNL processor consists of 64–72 cores with low base frequency (1.3–1.5 GHz). KNL offers AVX-512, a vector instruction set for 512-bit data words, which allows parallel computation on 16 single or 8 double precision floats. It also supports vector FMA (fused multiply-add) instructions (e.g., $d = ab + c$) for further fine-grained parallelism. Each core can issue two such instructions per cycle, which yields a theoretical single precision peak performance of 64 floating point operations (flops) per cycle. The KNL cores are joined in pairs called tiles located on a 2D mesh. Each core has its own 32 KB L1 cache and each tile has a 1 MB L2 cache. The latter supports two reads and one write every two cycles. This bandwidth is shared between two cores. Each core can host up to four hardware threads. KNL comes with two types of memory: up to 384 GB of DRAM (6 channels with an aggregate bandwidth of 80 GB/s as measured with the STREAM benchmark [30]) and 16 GB of high-bandwidth MCDRAM (8 channels and up to 440 GB/s respectively). The MCDRAM is configurable to work in one of three different modes: 1) *cache mode* in which it is used as L3 cache, 2) *flat mode* in which it serves as a scratchpad, i.e., a software-controlled memory (in this mode, there is no L3 cache), 3) *hybrid mode* in which part is working in cache mode and part in flat mode. In this paper, we use a KNL with 72 cores, 1.5 GHz base frequency, and 192 GB of DRAM in flat mode. The flat mode allows us to clearly separate the memory needed by the subtasks characterized in the next section.

3 METHOD DESCRIPTION

Our scheme uses block asynchronous coordinate descent with duality-gap based selection described in Section 2.2. The workflow, as illustrated in Figure 1, can be described as two tasks \mathcal{A} and \mathcal{B} running in parallel. Task \mathcal{A} is responsible for computing duality gap values gap_i based on the current model α and the shared vector \mathbf{v} . These values are then stored in a vector $\mathbf{z} \in \mathbb{R}^n$ which we call gap memory. In parallel to task \mathcal{A} , task \mathcal{B} performs updates on a subset of coordinates, which are selected based on their importance measure. As a solver we opt to use the parallel asynchronous stochastic coordinate descent (SCD). Since \mathcal{B} operates only on batches of data, it is typically faster than \mathcal{A} . Therefore, it is very likely that \mathcal{A} is not able to update all gaps during a single \mathcal{B} execution and some entries of the gap memory become stale as the algorithm proceeds. In practice, the algorithm works in epochs. In each epoch, \mathcal{B} performs an update on the batch of selected coordinates, where each coordinate is processed exactly once. At the same time, \mathcal{A} randomly samples coordinates and computes gap_i with the most recent (i.e., obtained in the previous epoch) parameters α, \mathbf{v} and updates the respective coordinate z_i of the gap memory. As soon as the work of \mathcal{B} is completed, it returns the updated α and \mathbf{v} to \mathcal{A} . \mathcal{A} pauses its execution to select a new subset of coordinates to send to \mathcal{B} , based on the current state of the gap memory \mathbf{z} . The robustness to staleness in the duality gap based coordinate selection scheme has empirically been shown in [15].

3.1 Implementation challenges

We identify the most computationally expensive parts of the proposed scheme. First, let us consider task \mathcal{A} ; the computation of the

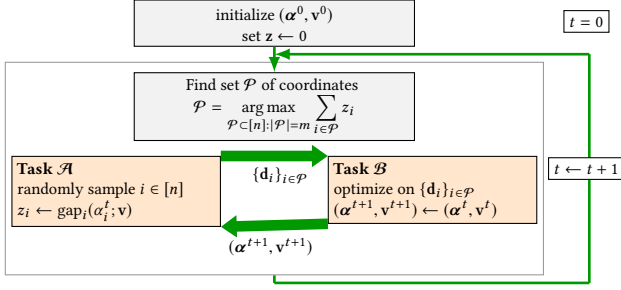


Figure 1: Visualization of the HTHC approach.

coordinate-wise duality gaps (2) involves an inner product computation between \mathbf{w} , computed from \mathbf{v} , and the respective data column \mathbf{d}_i :

$$z_i = h(\langle \mathbf{w}, \mathbf{d}_i \rangle, \alpha_i), \quad (3)$$

where h is a scalar function defined by the model; its evaluation cost is negligible.

Task \mathcal{B} performs the coordinate descent on the selected subset of the data. Thus, in each iteration of the algorithm, a coordinate descent update on one entry of α is performed, i.e., $\alpha_i^+ = \alpha_i + \delta$. Again this update takes the form

$$\delta = \hat{h}(\langle \mathbf{w}, \mathbf{d}_i \rangle, \alpha_i), \quad (4)$$

where \hat{h} is a scalar function. Note that the optimal coordinate update has a closed-form solution [37, 39] for many applications of interest, and otherwise allows a simple gradient-step restricted to the coordinate i . With every update on α we also update \mathbf{v} accordingly, i.e., $\mathbf{v}^+ = \mathbf{v} + \delta \mathbf{d}_i$, to keep these vectors consistent. The asynchronous implementation of SCD introduces additional challenges: staleness of the model information \mathbf{v} used to compute updates. This might slow down convergence or even lead to divergence for a large number of parallel updates. Additionally, writing to shared data requires synchronization, and generates write-contention which needs to be handled by appropriate locking.

4 IMPLEMENTATION ON MANYCORE PROCESSORS

The main contribution of this paper is to show that a scheme for learning GLMs based on multiple heterogeneous tasks is an efficient solution for implementation on a standalone, state-of-the-art manycore system such as KNL. As we will see, our approach is typically over an order of magnitude faster than simple C++ code with basic OpenMP directives. Due to the need for careful synchronization, locking and separation of resources, a straightforward implementation is not efficient in the manycore setting: a detailed calibration to the hardware resources and an associated implementation with detailed thread control is the key. In the following we will detail the challenges and key features for achieving an efficient implementation.

4.1 Parallelization of the workload

Our implementation uses four levels of parallelism: 1) \mathcal{A} and \mathcal{B} are executed in parallel. 2) \mathcal{A} performs updates of z_i in parallel and \mathcal{B} performs parallel coordinate updates. 3) \mathcal{B} uses multiple threads

for each vector operation. 4) The main computations are vectorized using AVX-512.

4.1.1 Allocation of resources to the tasks. To map HTHC onto the KNL we split compute and memory resources among the two tasks \mathcal{A} and \mathcal{B} . We split the compute resources by assigning separate sets of cores (in fact tiles for better data sharing) to each task. The respective number of cores is a parameter that makes our implementation adaptive to the problem and target platform. To achieve parallelism we use the threading library *pthread*, which provides the fine-grained control over thread affinity, synchronization, and locking over critical regions of the code. For more details we refer to Section 4.4. To split the memory resources between the two tasks we use the KNL in flat mode where the MCDRAM memory serves as a scratchpad. This setting is particularly suited for our scheme because we can allocate the data for \mathcal{A} to DRAM and the data for \mathcal{B} to MCDRAM. As a consequence, saturating the memory bandwidth by one task will not stall the other.

4.1.2 Parallelization of the tasks. In this section we discuss the fine-grained parallelization of the individual tasks performed by \mathcal{A} and \mathcal{B} . For \mathcal{A} , we use only one thread for every update of a single z_i . We do this due to high risk of deadlocks when computations on \mathcal{B} are finished and \mathcal{A} receives a signal to stop. For parallelism across threads, we perform several updates in parallel. The number $T_{\mathcal{A}}$ of threads used on \mathcal{A} is a parameter used for adaptation.

In contrast, task \mathcal{B} performs $T_{\mathcal{B}}$ updates in parallel and also parallelizes the inner product computation of each update across $V_{\mathcal{B}}$ threads. Thus, the total number of threads used by \mathcal{B} is $T_{\mathcal{B}} \cdot V_{\mathcal{B}}$. Both are parameters in our implementation. When $V_{\mathcal{B}}$ threads are used per update, \mathbf{v} and the corresponding \mathbf{d}_i are split into equal chunks. A simple model can be used to determine a good choice for $V_{\mathcal{B}}$ through a suitable chunk size as explained next.

As previously mentioned, the performance of both the inner product and the \mathbf{v} update is limited by the memory bandwidth. For this reason, it is desirable that \mathbf{v} , which is reused, stays in cache. To achieve this, the cache has to hold \mathbf{v} and two \mathbf{d}_i columns. Since \mathbf{v} and the \mathbf{d}_i have the same length, this means the chunk size should be about a third of the cache size, i.e., about 87,000 single precision numbers for the L2 caches in KNL. Optimizing with the same reasoning for the 32KB L1 cache would yield a length of \mathbf{v} below 4096 elements. Such short vectors would not benefit from parallelism due to issues discussed later. The best choice for $T_{\mathcal{B}}$ is influenced by several factors as will be discussed in Section 4.4.

4.1.3 Vectorization with AVX-512. We implemented both the scalar product (executed on both \mathcal{A} and \mathcal{B}) and the incrementation of \mathbf{v} (performed on \mathcal{B}) using AVX-512 FMA intrinsics with multiple accumulators for better instruction-level parallelism. The peak single core performance of KNL is 64 flops/cycle, but in the scalar product, each FMA requires two loads from L2 cache, reducing the peak to 16. In practice, our entire coordinate update achieves about 7.2 flops/cycle, about three times faster than without AVX.

4.2 Synchronization

Task \mathcal{A} does not write to shared variables and thus requires no synchronization between threads. In contrast, the updates on \mathcal{B} are performed with multiple threads per vector as explained in

the previous paragraph. For the updates of the form shown in (4), three barriers are required to separate the resetting of the shared result from the $\langle \mathbf{w}, \mathbf{d}_i \rangle$ calculation of a new scalar product and the computation of \hat{h} based on the new shared result.

For the implementation we use pthreads which provides synchronization mechanisms with mutexes and thread barriers. Since barriers are relatively expensive, we replace them with a mechanism based on integer counters protected by mutexes similar to [18].

In addition to synchronization per thread, we need to coordinate running and stopping the tasks at the beginning and the end of each epoch t (as presented in Fig. 1). To avoid the overhead of creating and destroying threads, we use a thread pool with a constant number of threads for \mathcal{A} and \mathcal{B} . To synchronize, we use another counter-based barrier scheme similar to the one described above.

4.3 Atomic operations

In our asynchronous coordinate descent implementation we enforce atomic updates to the shared vector \mathbf{v} in order to preserve the primal-dual relationship between \mathbf{w} and α and thus maintain strong convergence guarantees derived by Hsieh et al. [22]. The pthreads library does not provide atomic operations, but the mutexes can be used to lock chosen variables. Since locking every single element of the vector separately creates an enormous overhead, we use medium-grained locks for chunks of 1024 vector elements.

4.4 Balancing compute resources

A major challenge posed by the implementation of HTHC is how to balance the computing power across the different levels of parallelism as discussed in Section 4.1. The configuration of HTHC is parameterized by $T_{\mathcal{A}}$, $T_{\mathcal{B}}$, and $V_{\mathcal{B}}$, and can be adjusted to the hardware and problem at hand. We identified two important factors that impact the optimal setting:

(1) *Balanced execution speed.* If \mathcal{B} works significantly faster than \mathcal{A} , the latter executes too few z_i updates and most coordinate importance values become stale, thus, convergence suffers. This effect has empirically been investigated by Dünner et al. [15] who showed that satisfactory convergence can be obtained up to about 15% of the z_i being updated in each epoch while a smaller ration significantly degrades convergence. We will discuss this further in Section 5. On the other hand, if \mathcal{B} is too slow, the runtime suffers. As a consequence, the best balance depends also on the efficiency of the implementation and we therefore tune the best configuration.

(2) *Cache coherence.* The parallelization of the updates on \mathcal{A} requires no synchronization between caches, however, a large number of threads leads to DRAM bandwidth saturation. Additionally, more threads mean higher traffic on the mesh, which can impact the execution speed of \mathcal{B} . For fast convergence, the threads must be assigned so that \mathcal{A} performs a sufficient fraction of z_i updates in each epoch. Our results will confirm 15% as a safe choice.

Performance model. Recall that we operate on the data matrix $D \in \mathbb{R}^{d \times n}$, where each of the n coordinates corresponds to a column represented by vector \mathbf{d}_i of length d . Let m denote the number of coordinates processed by task \mathcal{B} per epoch. Let $t_{I,d}(\dots)$ denote the time of a single coordinate update on task $I \in \{\mathcal{A}, \mathcal{B}\}$ with vector length d . This function is not trivial to derive, due to relatively poor

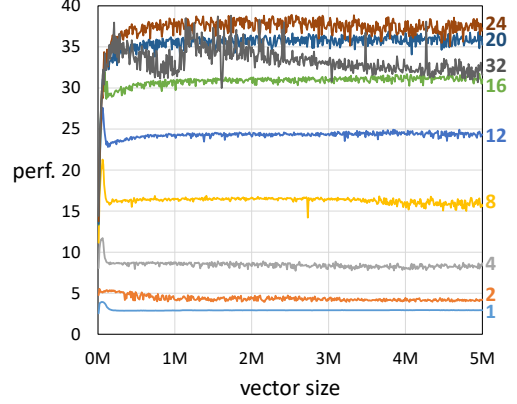


Figure 2: Performance (in flops/cycle) of synthetic \mathcal{A} operations. Different labels represent different values of $T_{\mathcal{A}}$.

scalability of the operations used and dependence on memory and synchronization speed. The values for all reasonable thread setups and lengths d can be calculated in advance and stored for future reference. The code will include precomputed values for different $t_{I,d}$. For fast convergence, we propose the following model for the parameters (d, n, \tilde{r} are constants):

$$\min_{m, T_{\mathcal{A}}, T_{\mathcal{B}}, V_{\mathcal{B}}} m \cdot t_{\mathcal{B},d}(T_{\mathcal{B}}, V_{\mathcal{B}}) \quad \text{s.t.} \quad \frac{m \cdot t_{\mathcal{B},d}(T_{\mathcal{B}}, V_{\mathcal{B}})}{t_{\mathcal{A},d}(T_{\mathcal{A}})} \geq \tilde{r} \cdot n \quad (5)$$

The values of $t_{I,d}$ need to be obtained once, during the installation, and saved in a table. This table can be later used by HTHC to quickly solve the problem.

5 EXPERIMENTAL RESULTS

We perform two series of experiments. In the first series, we create a benchmarking code on synthetic data, aimed to understand and illustrate how the different implementation parameters impact the performance of HTHC. In the second series, we compare HTHC on KNL against a number of more straightforward variants of implementing the same algorithm including standard C++ code with OpenMP directives.

All experiments are run on a KNL in flat mode as described in Section 2.3. We compile our code with the Intel Compiler Collection and flags `-std=c++11 -pthread -lmemkind -lnuma -O2 -xCOMMON-AVX512 -qopenmp`. In all experiments, we use at most one thread per core and single precision.

5.1 Algorithm profiling

To simulate different values of $t_{I,d}$ for different vector size d (details in Section 4.4), we imitate the expensive operations of the tasks \mathcal{A} and \mathcal{B} on synthetic data D . The code measures the overall time and performance for different vector sizes and thread numbers. The operations involve the data matrix D of size $n \times d$ and the shared vector \mathbf{v} , with threading and synchronization implemented as described in Section 4. In the following we will illustrate the performance of different aspects of our code for varying data size ($n = 600$ and d ranging from 10,000 to 5,000,000).

To analyze the impact of the parameter $T_{\mathcal{A}}$ on the performance of task \mathcal{A} , we allocate both data structures to DRAM and measure

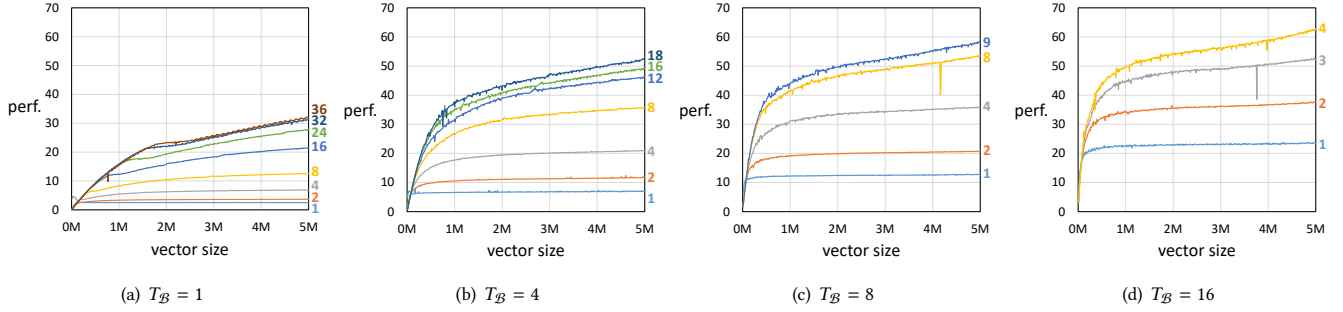


Figure 3: Performance (in flops/cycle) of operations of task \mathcal{B} for different numbers $T_{\mathcal{B}}$ of parallel updates. Different labels represent different values of $V_{\mathcal{B}}$.

performance for $T_{\mathcal{A}}$ ranging from 1 to 72. The results are presented in Fig. 2. We observe that above 20 parallel updates, the performance does not increase significantly and above 24 it even begins to decrease and fluctuate due to the saturation of DRAM bandwidth. For this reason, we use at most 24 threads for \mathcal{A} .

To analyze the impact of the parameter $V_{\mathcal{B}}$ and $T_{\mathcal{B}}$ on the performance of task \mathcal{B} , we allocate D and \mathbf{v} to MCDRAM. Fig. 3 illustrates the impact of $V_{\mathcal{B}}$ and shows results for $T_{\mathcal{B}} = \{1, 4, 8, 16\}$. The rapid drops in performance observable for large numbers of threads are caused by background processes which stall the execution of the program on particular cores. We note that below 130,000 it is best to use one thread per vector, independent of the number of parallel updates. For larger vectors, the best strategy is to use as many threads per vector as possible. We observe that for the vector lengths considered, higher performance is obtained with more parallel updates rather than more threads per vector.

Fig. 4 shows the speedup of isolated \mathcal{B} runs with different values of $T_{\mathcal{B}}$ over a run with $T_{\mathcal{B}} = 1$. For each value of $T_{\mathcal{B}}$, we plot results for the runs with the best corresponding $V_{\mathcal{B}}$. We observe that the algorithm used by \mathcal{B} does not scale well. This is due to many synchronization points during updates. Profiling with Intel VTune shows that while the bandwidth of L2 caches is a bottleneck on each tile, the saturation of MCDRAM bandwidth remains low. For this reason, we benefit from the flat mode, which keeps MCDRAM as a separate allocation space. The raw update speed of \mathcal{B} , contrary to the convergence of the complete scheme, is not affected by too many parallel updates of \mathbf{v} . In practice, the optimal value for $T_{\mathcal{B}}$ is rarely the maximum, as we will see in the following experiments.

5.2 Performance evaluation

The second series of experiments compares the performance of HTHC to several reference schemes of the two selected linear models across three data sets of different size. We consider Lasso and SVM on the three dense data sets in Table 1. Dogs vs. Cats features were extracted as in [20] and the number of samples was doubled. The same pre-processing was used in [15]. The News20 data set was artificially made dense by representing all features, both zero and non-zero, as vector elements. The regularization parameter λ was obtained to provide a support size of 12% for Lasso on Epsilon and Dogs vs. Cats, and using cross validation in all other cases.

Table 1: Data sets used in the experiments

Data set	Samples	Features	Approx. size (GB)
Epsilon [24]	400,000	2,000	3.2
Dogs vs. Cats [20]	40,002	200,704	32.1
News20 [16]	19,996	1,355,191	108.4

5.2.1 Comparison to our baselines. In the following we will denote HTHC as $\mathcal{A} + \mathcal{B}$ emphasizing that it runs two tasks, \mathcal{A} and \mathcal{B} . As detailed in Section 4.1.1, HTHC allocates the data for \mathcal{A} to DRAM and the data for \mathcal{B} to MCDRAM. For each experiment, we used exhaustive search to find the best parameter settings, i.e., percentage of data updated by \mathcal{B} per epoch $\%_{\mathcal{B}}$, and the thread settings $T_{\mathcal{A}}, T_{\mathcal{B}}, V_{\mathcal{B}}$ described in Section 4. These are presented in Tables 3, 4. We compare HTHC against four reference implementations:

- (1) ST: We consider a homogeneous single task implementation, which allocates the data matrix D to DRAM and the remaining data to MCDRAM. It performs cyclic asynchronous CD with randomized update order. The same low-level optimizations are used for this implementation than in task \mathcal{B} of HTHC but without duality-gap-based coordinate selection. Instead, in each epoch it updates \mathbf{v}, α (allocated to MCDRAM) for all coordinates of D . Again, we run a search for the best parameters. These are shown in Tables 3 and 4.
- (2) ST ($\mathcal{A} + \mathcal{B}$): For comparison, we also run ST with the setting of $T_{\mathcal{B}}$ and $V_{\mathcal{B}}$ as found in $\mathcal{A} + \mathcal{B}$.
- (3) OMP: We include what one could call a straightforward implementation: standard looped C code using the OpenMP directives `simd` reduction and `parallel` for for parallelization with the thread counts $T_{\mathcal{B}}$ and $V_{\mathcal{B}}$ of ST. The code performs the same operations as $\mathcal{A} + \mathcal{B}$. To lock \mathbf{v} elements, we use directive `atomic`.
- (4) OMP WILD is the same as OMP, but the operations on \mathbf{v} are lock-free (without `atomic`).

Fig. 5 shows the results for Lasso and SVM for each data set. Each plot shows the precision of the algorithm versus the running time. For Lasso, we measure suboptimality, for Lasso and SVM we

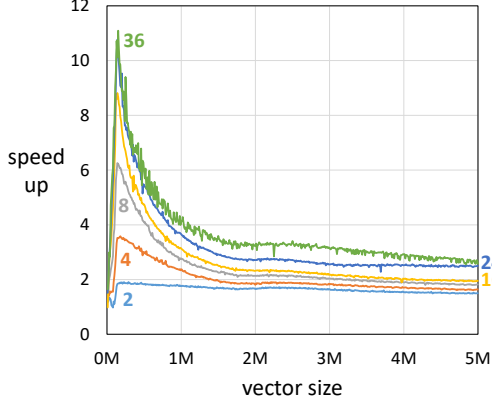


Figure 4: Speedup of runs with different number T_B of parallel updates over runs with a single update on \mathcal{B} .

show the duality gap.¹ Each algorithm is run until the duality gap reaches 10^{-5} or until timeout.

First, we discuss the $\mathcal{A} + \mathcal{B}$, ST, and ST ($\mathcal{A} + \mathcal{B}$). For all Lasso runs, we observe a speedup varying from about $5\times$ for Epsilon to about $10.7\times$ for News20 compared to the best ST run, depending on the desired precision. As expected, ST ($\mathcal{A} + \mathcal{B}$) is never better than ST since the latter uses the best parameters found during the search. The results for suboptimality are consistent with those for the duality gaps.

For the SVM runs, we achieve $3.5\times$ speedup for Dogs vs. Cats and competitive performance for Epsilon, however, for News20 we observe that the ST implementations beat $\mathcal{A} + \mathcal{B}$. A possible explanation is that the duality gaps of different coordinates are similar, and fall in and out of \mathcal{B} 's working set frequently, slowing down identification of the support vectors. For News20, ST converges within ca. 10 epochs, while $\mathcal{A} + \mathcal{B}$ takes more than 150 epochs. This might suggest that even for the best thread setup found, \mathcal{B} is too fast compared to \mathcal{A} . It might be beneficial to increase the workload of \mathcal{B} by enabling multiple updates per coordinate in the same epoch.

Next we discuss the OpenMP runs. For OMP, as expected, the atomic operations severely impact performance. On the other hand, OMP WILD is much faster than OMP (due to no overhead of atomic operations) but does not guarantee the primal-dual relationship between \mathbf{w} and $\boldsymbol{\alpha}$ and thus does not converge to the exact minimizer; hence the plateau in the figures presenting suboptimality. The duality gap computation $\text{gap}_i(\alpha_i; \hat{\mathbf{w}})$ is based on $\hat{\mathbf{v}} \neq D\boldsymbol{\alpha}$, and thus do not correspond to the true values: therefore, the gap of OMP WILD eventually becomes smaller than suboptimality. For SVM, OMP WILD performs competitive with $\mathcal{A} + \mathcal{B}$ on Epsilon, and even faster than $\mathcal{A} + \mathcal{B}$ for News20, however, it converges only to an approximate solution.

5.2.2 Comparison against other parallel CD implementations. The work [15] implements a similar scheme for parallelizing SCD on a heterogeneous platform: an 8-core Intel Xeon E5 x86 CPU with NVIDIA Quadro M4000 GPU accelerator (we note that this

is a relatively old GPU generation: the newer accelerators would give better results). It provides results for Dogs vs. Cats with \mathcal{B} updates set to 25% (the largest size that fits into GPU RAM): a suboptimality of 10^{-5} is reached in 40 seconds for Lasso and a duality gap of 10^{-5} is reached in about 100 seconds for SVM. With the same percentage of \mathcal{B} updates, HTHC needs 29 and 84 seconds, respectively. With our best setting (Figs. 5(d)– 5(f)) this is reduced to 20 and 41 seconds, respectively. In summary, on this data, our solution on the standalone KNL is competitive with a state-of-the-art solution using a GPU accelerator with many more cores. We also show that its performance can be greatly improved with proper number of updates on \mathcal{B} .

Additionally, we compare the SVM runs of HTHC ($\mathcal{A} + \mathcal{B}$) and our parallel baseline (ST) against PASSCoDe [22], a state-of-the-art parallel CD algorithm. We compare against the variant with atomic lock on \mathbf{v} (PASSCoDe-atomic) and a lock-free implementation (PASSCoDe-wild) which is faster, but does not maintain relationship between model parameters as discussed in Section 4.3. The results are presented in Table 2. On Epsilon, the time to reach 85% accuracy with 2 threads (the same as T_B for ST) is 8.6 s for PASSCoDe-atomic and 3.21 s for PASSCoDe-wild, but these times decrease to 0.70 s with 24 threads and 0.64 s with 12 threads respectively. For Dogs vs. Cats, greatly increasing or decreasing the T_B compared to ST did not improve the result. Running on the dense News20 dataset was not possible due to excessive storage space required by PASSCoDe utils when parsing files in LIBSVM format. Table 2 shows that for Dogs vs. Cats, we are $2.4\text{--}5\times$ faster, depending on the versions we compare. For Epsilon, we are roughly $2\times$ faster, but exploiting the the HTHC design is required to prevent slowdown.

5.3 Experiments on sensitivity

During the search for $\mathcal{A} + \mathcal{B}$, four parameters were considered: size of \mathcal{B} , T_A , T_B and V_B . Our goal was not only to find the best parameters, but also identify parameters giving a close-to-best solution. Figs. 6 present parameters which provided no more than overall 110% convergence time of the best solution found. The overall convergence time depends on the number of epochs which varies from run to run for the same parameters: therefore, we consider all the presented parameters capable of obtaining the minimum runtime. The plots present four dimensions: the axes correspond to T_B and V_B while different markers correspond to different $\%_B$. The labels next to the markers correspond to T_A . The color of each label corresponds to its marker. Multiple values per label are possible. To save time during the search, for Dogs vs. Cats we use a step of 4 for T_A and a step of 2 for T_B . We also note that while Lasso on Epsilon converges fast for T_B greater than 8, the rate of diverging runs is too high to consider it for practical application.

To examine how the number of \mathcal{A} updates per epoch affects the convergence, we group the successful runs of the parameter search by the number of z_i updated by \mathcal{A} and check how many epochs were required to converge on average, and the average time to converge. We present example results in Figs. 7. We observe that relatively few updates are needed for the best average speed: 15% for Epsilon and 10% for Dogs vs. Cats. While these runs need more

¹ to compute the duality gap for Lasso we use the Lipschitzing trick as proposed by Dünner et al. [14].

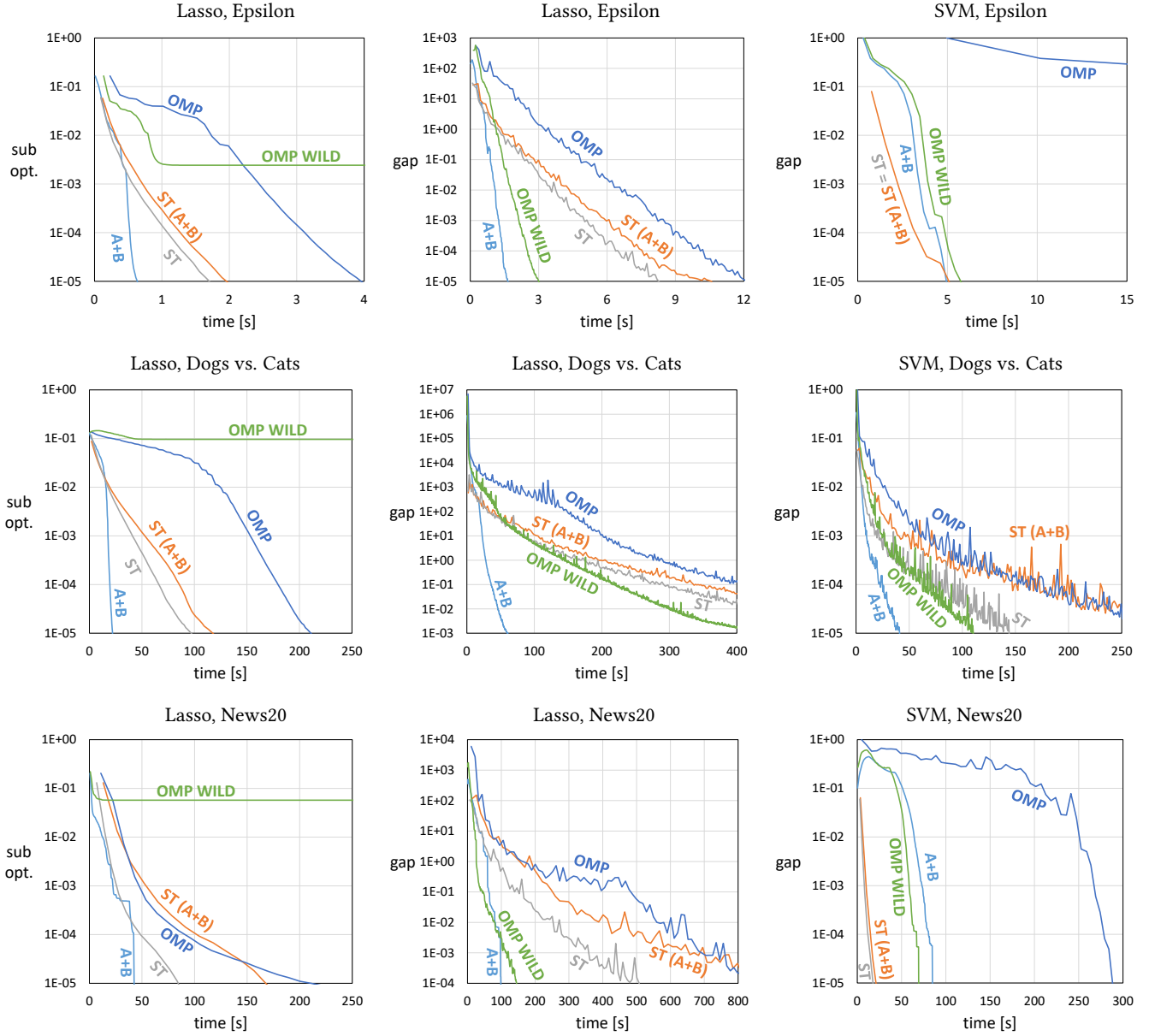


Figure 5: Convergence for Epsilon, Dogs vs. Cats and News20.

Table 2: Comparison of $\mathcal{A} + \mathcal{B}$ and ST against PASSCoDe

Data set	Accuracy	HTHC	ST	PASSCoDe- atomic	PASSCoDe- wild
Epsilon	85%	0.35 s	1.11 s	0.70 s	0.64 s
Dogs vs. Cats	95%	0.51 s	0.69 s	2.69 s	1.66 s

Table 3: Best parameters found for Lasso.

Data set	λ	settings for $\mathcal{A} + \mathcal{B}$					settings for ST		
		$\% \mathcal{B}$	$T_{\mathcal{A}}$	$T_{\mathcal{B}}$	$V_{\mathcal{B}}$	T_{total}	$T_{\mathcal{B}}$	$V_{\mathcal{B}}$	T_{total}
Epsilon	0.0003	9%	16	6	9	70	8	9	72
Dogs vs. Cats	0.0025	4%	16	14	1	30	20	1	20
News20	0.0001	3%	12	6	1	18	60	1	60

epochs to converge, the epochs are executed fast enough to provide optimal overall convergence speed.

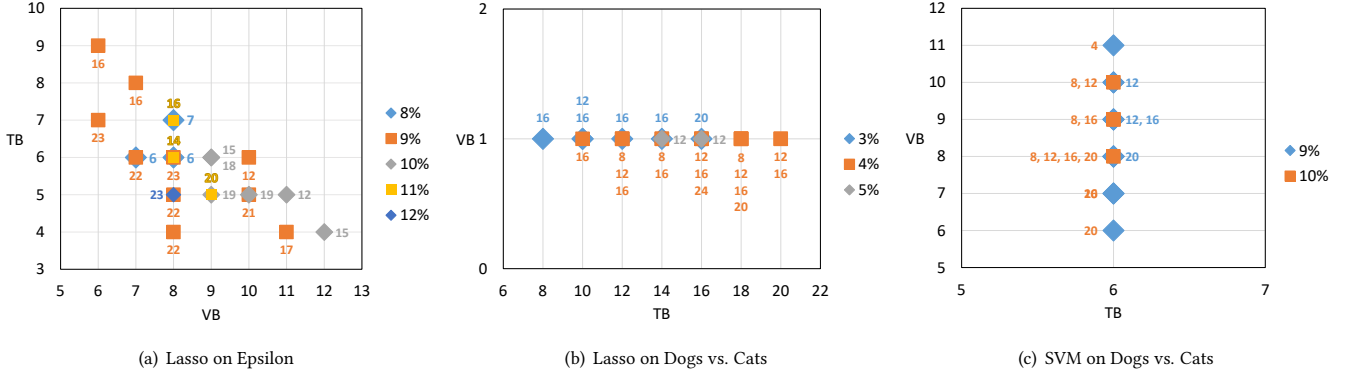


Figure 6: Parameter combinations (T_B , V_B) providing fast convergence (within 110% time of the best found).

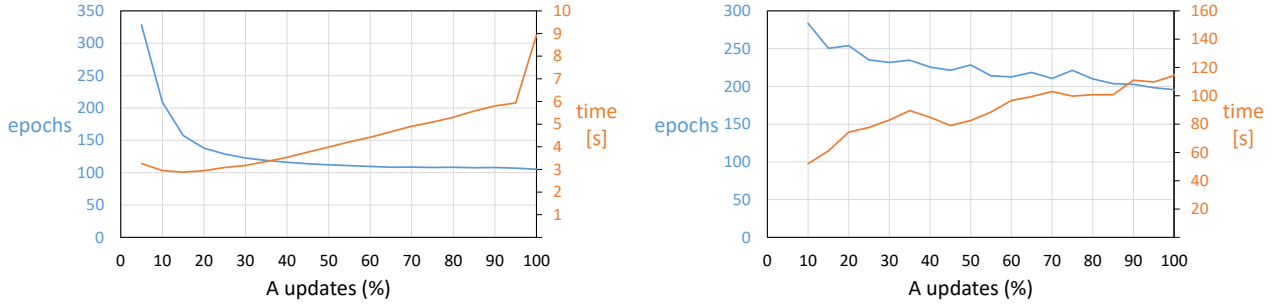


Figure 7: Sensitivity to the number of \mathcal{A} updates per epoch for (left) Lasso on Epsilon and (right) SVM on Dogs vs. Cats.

Table 4: Best parameters found for SVM

Data set	λ	settings for $\mathcal{A} + \mathcal{B}$					settings for ST		
		% \mathcal{B}	$T_{\mathcal{A}}$	$T_{\mathcal{B}}$	$V_{\mathcal{B}}$	T_{total}	$T_{\mathcal{B}}$	$V_{\mathcal{B}}$	T_{total}
Epsilon	0.0001	18%	20	2	1	22	2	1	2
Dogs vs. Cats	0.0001	9%	20	6	7	62	36	2	72
News20	0.001	10%	20	20	2	60	14	4	56

6 RELATED WORK

Variants of stochastic coordinate descent [40] have become the state-of-the-art methods for training GLMs on parallel and distributed machine learning systems. Parallel coordinate descent (CD) has a long history, see e.g. [35] and recent research has contributed to asynchronous variants such as [22, 25, 26]. PaSSCoDe [22] is a family of asynchronous parallel CD algorithms for ℓ_2 -regularized problems. In [22], dual variables are updated in parallel, under three approaches: locking the vector \mathbf{v} , using atomic operations and a lock-free implementation are shown to converge for small block size. For large block size, the algorithm is reported to diverge. This problem can be mitigated by techniques proposed by Zhang and Hsieh [47]. Parallel CD has also been studied beyond ℓ_2 regularized problems, see e.g. [7].

On non-uniform memory systems (memory and disk) dual CD was studied for the SVM problem by selectively loading samples [9]

and also in a more general setting with random (block) coordinate selection [29]. In a single machine setting, various schemes for selecting the relevant coordinates for CD have been studied, including adaptive probabilities [13, 32, 38] or fixed importance sampling [48]. The selection of relevant coordinates can be based on the steepest gradient, e.g. [21, 43], Lipschitz constant of the gradient [46], nearest neighbor [41] or duality gap based measures [15] as used in this work.

Regarding manycore machine learning, current machines, including KNL, are already widely used for deep learning, as standalone devices or within clusters [12, 19, 23, 28, 42]. A notable example is using TACC Stampede 2 cluster ² with a world record in training speed of ImageNet [45]. SVM training on multicore and manycore architectures was proposed by You et al. [44]. The authors provide evaluation for Knights Corner (KNC) and Ivy Bridge, proving them to be competitive with GPUs. The LIBSVM library [8] is implemented for both GPU [4] and KNC [27]. All SVM implementations use the sequential minimization algorithm [33]. For training on large-scale linear models, a multi-core extension of LIBLINEAR [17] was proposed by Chiang et al. [11]. Rendle et al. [34] introduced coordinate descent for sparse data on distributed systems, achieving almost linear scalability: their approach can be applied to multi- and manycore. For k-means, a framework for manycore systems [5] as well as a KNL-specific implementation [3] are discussed. The latter

²portal.tacc.utexas.edu/user-guides/stampede2

reports a $22\times$ speedup from the usage of AVX-512 and multithreading. Abdulah et al. [2] consider maximum-likelihood estimation on Intel processors, however, they show that an 18-core Haswell processor outperforms KNL.

7 CONCLUSIONS

We introduced HTHC for training general linear models on standalone manycore computers including a complete, architecture-cognizant implementation. We showed that it provides a significant reduction of training time as opposed to a straightforward implementation of coordinate descent. In our experiments, the speedup varies from $5\times$ to more than $10\times$ depending on the data set as well as the stopping criterion. We also showed that an implementation on a 72-core machine, even when using only a fraction of its resources, is competitive against a CPU-GPU system with more than 1500 GPU cores. An advantage of HTHC over the CPU-GPU heterogeneous learning schemes is the ability of balancing distribution of machine resources such as memory and CPU cores between different tasks, an approach inherently impossible on heterogeneous platforms. To the best of our knowledge, this is the first such scheme proposed in the field of manycore machine learning. The inherent adaptivity of HTHC should enable porting it to other existing and future standalone manycore platforms.

REFERENCES

- [1] Martín Abadi, Paul Barham, Jianmin Chen, Zhifeng Chen, Andy Davis, Jeffrey Dean, Matthieu Devin, Sanjay Ghemawat, Geoffrey Irving, Michael Isard, et al. 2016. TensorFlow: A System for Large-Scale Machine Learning.. In *OSDI*, Vol. 16. 265–283.
- [2] Sameh Abdulah, Hatem Ltaief, Ying Sun, Marc G Genton, and David E Keyes. 2018. Tile Low-Rank Approximation of Large-Scale Maximum Likelihood Estimation on Manycore Architectures. *arXiv preprint arXiv:1804.09137* (2018).
- [3] Abdullah Al Hasib, Juan M Cebrian, and Lasse Natvig. 2018. A vectorized k-means algorithm for compressed datasets: design and experimental analysis. *The Journal of Supercomputing* (2018), 1–24.
- [4] Andreas Athanasiopoulos, Anastasios Dimou, Vasileios Mezaris, and Ioannis Kompatsiaris. 2011. GPU acceleration for support vector machines. In *Proc. 12th Inter. Workshop on Image Analysis for Multimedia Interactive Services (WIAMIS 2011)*, Delft, Netherlands.
- [5] Christian Böhm, Martin Perdacher, and Claudia Plant. 2017. Multi-core K-means. In *Proceedings of the 2017 SIAM International Conference on Data Mining*. SIAM, 273–281.
- [6] Stephen P Boyd and Lieven Vandenbergh. 2004. *Convex optimization*. Cambridge University Press.
- [7] Joseph K. Bradley, Aapo Kyrola, Danny Bickson, and Carlos Guestrin. 2011. Parallel Coordinate Descent for L1-Regularized Loss Minimization. *CoRR* abs/1105.5379 (2011).
- [8] Chih-Chung Chang and Chih-Jen Lin. 2011. LIBSVM: A Library for Support Vector Machines. *ACM Trans. Intell. Syst. Technol.* 2, 3 (May 2011), 27:1–27:27.
- [9] Kai-Wei Chang and Dan Roth. 2011. Selective Block Minimization for Faster Convergence of Limited Memory Large-scale Linear Models. In *Proceedings of the 17th ACM SIGKDD International Conference on Knowledge Discovery and Data Mining*. 699–707.
- [10] Sharan Chetlur, Cliff Woolley, Philippe Vandermersch, Jonathan Cohen, John Tran, Bryan Catanzaro, and Evan Shelhamer. 2014. cuDNN: Efficient Primitives for Deep Learning. *CoRR* abs/1410.0759 (2014).
- [11] Wei-Lin Chiang, Mu-Chu Lee, and Chih-Jen Lin. 2016. Parallel Dual Coordinate Descent Method for Large-scale Linear Classification in Multi-core Environments. In *Proceedings of the 22nd ACM SIGKDD International Conference on Knowledge Discovery and Data Mining*. 1485–1494.
- [12] Valeriu Codreanu, Damian Podareanu, and Vikram A. Salek. 2017. Scale out for large minibatch SGD: Residual network training on ImageNet-1K with improved accuracy and reduced time to train. *CoRR* abs/1711.04291 (2017).
- [13] Dominik Csiba, Zheng Qu, and Peter Richtárik. 2015. Stochastic Dual Coordinate Ascent with Adaptive Probabilities. In *Proceedings of the 32nd International Conference on Machine Learning - Volume 37 (ICML '15)*. 674–683.
- [14] Celestine Dünner, Simone Forte, Martin Takáč, and Martin Jaggi. 2016. Primal-dual Rates and Certificates. In *Proceedings of the 33rd International Conference on Machine Learning - Volume 48 (ICML '16)*. 783–792.
- [15] Celestine Dünner, Thomas Parnell, and Martin Jaggi. 2017. Efficient Use of Limited-Memory Accelerators for Linear Learning on Heterogeneous Systems. In *Advances in Neural Information Processing Systems*. 4258–4267.
- [16] Rong-En Fan. 2018. LIBSVM Data: Classification (Binary Class). Retrieved 2018-09-03 from www.csie.ntu.edu.tw/~cjlin/libsvmtools/datasets/binary.html
- [17] Rong-En Fan, Kai-Wei Chang, Cho-Jui Hsieh, Xiang-Rui Wang, and Chih-Jen Lin. 2008. LIBLINEAR: A Library for Large Linear Classification. *J. Mach. Learn. Res.* 9 (June 2008), 1871–1874.
- [18] Franz Franchetti. 2005. Fast Barrier for x86 Platforms. Retrieved 2018-09-03 from www.spiral.net/software/barrier.html
- [19] Nitin Gawande, Joshua B. Landwehr, Jeff A. Daily, Nathan R. Tallent, Abhinav Vishnu, and Darren J. Kerbyson. 2017. Scaling Deep Learning Workloads: NVIDIA DGX-1/Pascal and Intel Knights Landing. *2017 IEEE International Parallel and Distributed Processing Symposium Workshops (IPDPSW)* (2017), 399–408.
- [20] Christina Heinze, Brian McWilliams, and Nicolai Meinshausen. 2016. Dual-loco: Distributing statistical estimation using random projections. In *Artificial Intelligence and Statistics*. 875–883.
- [21] Cho-Jui Hsieh and Inderjit S. Dhillon. 2011. Fast Coordinate Descent Methods with Variable Selection for Non-negative Matrix Factorization. In *Proceedings of the 17th ACM SIGKDD International Conference on Knowledge Discovery and Data Mining*. 1064–1072.
- [22] Cho-Jui Hsieh, Hsiang-Fu Yu, and Inderjit Dhillon. 2015. PASSCoDe: Parallel ASynchronous Stochastic dual Co-ordinate Descent. In *International Conference on Machine Learning*. 2370–2379.
- [23] Daejin Jung, Sunjung Lee, Wonjong Rhee, and Jung Ho Ahn. 2018. Partitioning Compute Units in CNN Acceleration for Statistical Memory Traffic Shaping. *IEEE Computer Architecture Letters* 17, 1 (2018), 72–75.
- [24] Knowledge 4 All Foundation Ltd. 2008. Large Scale Learning Challenge. Retrieved 2018-09-03 from www.k4all.org/project/large-scale-learning-challenge/
- [25] Rémi Leblond, Fabian Pederegosa, and Simon Lacoste-Julien. 2018. Improved asynchronous parallel optimization analysis for stochastic incremental methods. *arXiv preprint arXiv:1801.03749* (2018).
- [26] Ji Liu, Stephen J. Wright, Christopher Ré, Victor Bittorf, and Srikrishna Sridhar. 2015. An Asynchronous Parallel Stochastic Coordinate Descent Algorithm. *J. Mach. Learn. Res.* 16, 1 (Jan. 2015), 285–322.
- [27] Renzo Massobrio, Sergio Nesmachnow, and Bernabé Dorronsoro. 2017. Support vector machine acceleration for Intel Xeon Phi manycore processors. In *Latin American High Performance Computing Conference*. Springer, 277–290.
- [28] Amrita Mathuriya, Thorsten Kurth, Vivek Rane, Mustafa Mustafa, Lei Shao, Debbie Bard, Prabhat, and Victor W. Lee. 2017. Scaling GRPC Tensorflow on 512 nodes of Cori Supercomputer. *CoRR* abs/1712.09388 (2017).
- [29] Shin Matsushima, S.V.N. Vishwanathan, and Alexander J. Smola. 2012. Linear Support Vector Machines via Dual Cached Loops. In *Proceedings of the 18th ACM SIGKDD International Conference on Knowledge Discovery and Data Mining*. 177–185.
- [30] John McCalpin. 1995. Memory bandwidth and machine balance in high performance computers. (12 1995), 19–25.
- [31] José MF Moura, Markus Püschel, David Padua, and Jack Dongarra. 2005. Special issue on program generation, optimization, and platform adaptation. *Proc. IEEE* 93, 2 (2005), 211–215.
- [32] Dmytro Perekhrenko, Volkan Cevher, and Martin Jaggi. 2017. Faster Coordinate Descent via Adaptive Importance Sampling. *Proceedings of the 20th International Conference on Artificial Intelligence and Statistics* 54 (2017).
- [33] John Platt. 1998. *Sequential Minimal Optimization: A Fast Algorithm for Training Support Vector Machines*. Technical Report.
- [34] Steffen Rendle, Dennis Fetterly, Eugene J. Shekita, and Bor-yiing Su. 2016. Robust Large-Scale Machine Learning in the Cloud. In *Proceedings of the 22nd ACM SIGKDD International Conference on Knowledge Discovery and Data Mining*. 1125–1134.
- [35] Peter Richtárik and Martin Takáč. 2016. Parallel coordinate descent methods for big data optimization. *Mathematical Programming* 156, 1-2 (2016), 433–484.
- [36] Frank Seide and Amit Agarwal. 2016. CNTK: Microsoft’s open-source deep-learning toolkit. In *Proc. International Conference on Knowledge Discovery and Data Mining (KDD)*. 2135–2135.
- [37] Shai Shalev-Shwartz and Tong Zhang. 2013. Stochastic dual coordinate ascent methods for regularized loss minimization. *Journal of Machine Learning Research* 14, Feb (2013), 567–599.
- [38] Sebastian U Stich, Anant Raj, and Martin Jaggi. 2017. Safe adaptive importance sampling. In *Advances in Neural Information Processing Systems*. 4381–4391.
- [39] Stephen J Wright. 2015. Coordinate descent algorithms. *Mathematical Programming* 151, 1 (March 2015), 3–34.
- [40] Stephen J Wright. 2015. Coordinate descent algorithms. *Mathematical Programming* 151, 1 (2015), 3–34.
- [41] Ian En-Hsu Yen, Chun-Fu Chang, Ting-Wei Lin, Shan-Wei Lin, and Shou-De Lin. 2013. Indexed Block Coordinate Descent for Large-scale Linear Classification

- with Limited Memory. In *Proceedings of the 19th ACM SIGKDD International Conference on Knowledge Discovery and Data Mining*. 248–256.
- [42] Yang You, Aydin Buluç, and James Demmel. 2017. Scaling deep learning on GPU and Knights Landing clusters. In *SC*.
 - [43] Yang You, Xiang Ru Lian, Ji Liu, Hsiang-Fu Yu, Inderjit S. Dhillon, James Demmel, and Cho-Jui Hsieh. 2016. Asynchronous Parallel Greedy Coordinate Descent. In *Proceedings of the 30th International Conference on Neural Information Processing Systems*. 4689–4697.
 - [44] Y. You, S. L. Song, H. Fu, A. Marquez, M. M. Dehnavi, K. Barker, K. W. Cameron, A. P. Randles, and G. Yang. 2014. MIC-SVM: Designing a Highly Efficient Support Vector Machine for Advanced Modern Multi-core and Many-Core Architectures. In *2014 IEEE 28th International Parallel and Distributed Processing Symposium*. 809–818.
 - [45] Yang You, Zhao Zhang, Cho-Jui Hsieh, and James Demmel. 2017. 100-epoch ImageNet Training with AlexNet in 24 Minutes. *CoRR* abs/1709.05011 (2017).
 - [46] Aston Zhang and Quanquan Gu. 2016. Accelerated Stochastic Block Coordinate Descent with Optimal Sampling. In *Proceedings of the 22Nd ACM SIGKDD International Conference on Knowledge Discovery and Data Mining*. 2035–2044.
 - [47] H. Zhang and C. J. Hsieh. 2016. Fixing the Convergence Problems in Parallel Asynchronous Dual Coordinate Descent. In *2016 IEEE 16th International Conference on Data Mining (ICDM)*. 619–628.
 - [48] Peilin Zhao and Tong Zhang. 2015. Stochastic Optimization with Importance Sampling for Regularized Loss Minimization. In *Proceedings of the 32nd International Conference on Machine Learning (Proceedings of Machine Learning Research)*, Vol. 37. 1–9.